Pose measurement method based on geometrical constraints

Zimiao Zhang (张子森)*, Changku Sun (孙长库), Pengfei Sun (孙鹏飞), and Peng Wang (王 鹏)

State Key Laboratory of Precision Measuring Technology and Instruments, Tianjin University, Tianjin 300072, China

**Corresponding author: zht8581@yahoo.com.cn*

Received December 21, 2010; accepted March 24, 2011; posted online June 16, 2011

The pose estimation method based on geometric constraints is studied. The coordinates of the five feature points in the camera coordinate system are calculated to obtain the pose of an object on the basis of the geometric constraints formed by the connective lines of the feature points and the coordinates of the feature points on the CCD image plane; during the solution process, the scaling and orthography projection model is used to approximate the perspective projection model. The initial values of the coordinates of the five feature points in the camera coordinate system are obtained to ensure the accuracy and convergence rate of the non-linear algorithm. In accordance with the perspective projection characteristics of the circular feature landmarks, we propose an approach that enables the iterative acquisition of accurate target poses through the correction of the perspective projection coordinates of the circular feature landmark centers. Experimental results show that the translation positioning accuracy reaches ±0.05 mm in the measurement range of 0–40 mm, and the rotation positioning accuracy reaches ±0.06° in the measurement range of 4°–60°.

OCIS codes: 150.0155, 140.1135, 330.4060.
doi: 10.3788/COL201109.081501.

Object pose estimation, which can be widely applied in fields such as robot navigation[1], surgery[2], electro-optic aiming systems[3], vehicle quality inspection[4], aerospace[5,6], etc, presents considerable value in these industries. Compared with the pose estimation method based on the magnetic field[7], the machine vision technique is widely studied because it enables the avoidance of electromagnetic interference. Among the machine vision methods, the monocular vision method elicits considerable attention for its advantages: a non-contact, simple structure, and fewer calibration steps[8−10].

Thus, research in this area has become more intensive in recent years. DeMenthon *et al.*[11] proposed the POSIT algorithm, which requires a higher degree of four non-coplanar feature points[11]. In Ref. [12], the rotation and translation matrix is solved using least squares method in accordance with orthonormal constraints that use an excessive number of points (10×10). In Ref. [13], four feature points have been verified to achieve a linear solution, but the four points may have more than one solution[14]. Tang *et al.* presented a linear algorithm in which five feature points were considered[15]; however, the linear method did not carefully consider the geometrical constraints. Heikkild *et al.* demonstrated a method for correcting asymmetric projection, but this method employed in camera calibration, inducing an additional coordinate system[16]. The perspective projection model of a circle uses a skewed cone, which requires substantial calculation.

In this letter, the position estimation method based on geometric constraints is investigated. The coordinates of the five feature points in the camera coordinate system is calculated to obtain the pose of an object on the basis of the geometric constraints formed by the connective lines of the feature points and the coordinates of the feature points on the change-coupled device (CCD) image plane. During the solution process, the scaling and orthography projection model is used to approximate the perspective projection model. The initial values of the coordinates of the five feature points in the camera coordinate system are obtained to ensure the accuracy and convergence rate of the non-linear algorithm. In accordance with the perspective projection characteristics of the circular feature landmarks (generally, the perspective projection point of a circular feature landmark center is not the center of the corresponding perspective projection image), we propose an approach that enables the iterative acquisition of accurate target poses through the correction of the perspective projection coordinates of the circular feature landmark centers.

The planar target pattern with five reference points is designed for position and orientation estimation (Fig. 1). The Nos. 2, 3, and 4 points are on the same straight line. The Nos. 1 and 0 points can be distinguished according to the distance between the point and the straight line. The No. 4 point is farthest from the straight line composed of the Nos. 0 and 1 points. The Nos. 2 and 3 points can be distinguished according to their distances from No. 4. The No. 0 point is set as the origin of the coordinate system, and the connecting line between Nos. 0 and 1 is the y-axis of the coordinate system. The direction

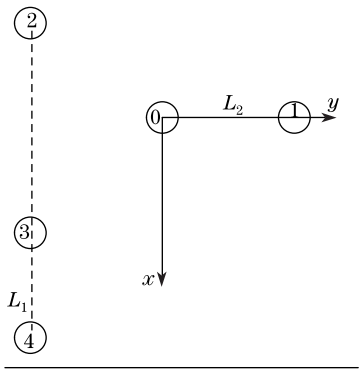

Fig. 1. Measurement target with five feature points.

parallel to the connecting line between Nos. 2 and 4 beginning downward from point No. 0 is the x-axis. The z-axis is determined in accordance with the principle of the right hand. The distance between each two points is known before positioning. Thus, the distance between each two reference points and the angle between every two vector of the reference points can be calculated.

To achieve the solution of the object pose, the coordinates of the feature points in the camera coordinate system require resolution. The perspective projection model of five feature points is shown in Fig. 2. $O_c - x_c y_c z_c$ is the camera coordinate system, which denotes the camera frame. uv is the CCD image plane with the original point at the image center of the CCD plane. The intrinsic parameters of the camera can be obtained through camera calibration in accordance with the robotic arm camera (RAC) calibration method presented by TSAI. These intrinsic parameters include the focus of lens f, the radial distortion coefficient of camera lens k, the center pixel of the computer image (u_0, v_0), and uncertainty image factor s_x. Because of the lens radial distortion, the undistorted coordinate point on the image plane can be obtained using the transformation formula of the ideal image coordinate and the actual image coordinates.

The coordinates of the feature points in the camera coordinate system are denoted by $P_i^c = (x_{ci}, y_{ci}, z_{ci})$, and the corresponding ideal image coordinates are denoted by $I_i = (x_{ui}, y_{ui})^T (i{=}0,\ 1,\ 2,\ 3,\ 4)$. The relationship between $\overrightarrow{O_c P_i^c}$ and $\overrightarrow{O_c I_i}$ can be described as

$$\overrightarrow{O_c P_i^c} = h_i \overrightarrow{O_c I_i}. \tag{1}$$

The coordinates of the feature points in the camera coordinate system can be obtained by solving h_i. The connective lines among feature points can constitute a geometric figure in space, and the solution of h_i is completed in accordance with the geometric constraints formed by the figure. The geometric constraints include lines, angles, and planes.

Figure 3 shows that the spatial geometric model of the figure enclosed by the connective lines of five feature points is known. The geometric figure includes C_5^3 triangles and each triangle has three sides. Each side of the triangle can be expressed as

$$\left|\overrightarrow{P_i P_j}\right|^2 = h_i^2 \left|\overrightarrow{O_c I_i}\right|^2 + h_j^2 \left|\overrightarrow{O_c I_j}\right|^2 - 2h_i h_j \overrightarrow{O_c I_i} \cdot \overrightarrow{O_c I_j}. \tag{2}$$

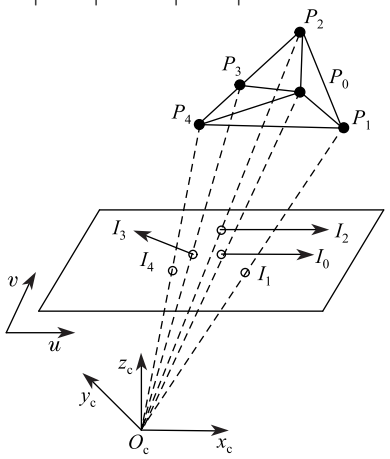

Fig. 2. Five-point perspective projection model.

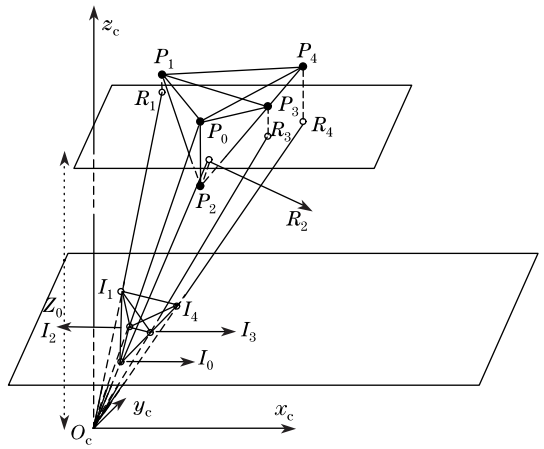

Fig. 3. Scaling and orthography projection model of five points.

There are 10 aggregate distance constraints.

Each triangle has three angles. Every four points can make up three pairs of vectors, and each pair of vectors can also constitute an angle. These angles can be denoted by

$$\begin{cases} \cos\angle P_i P_j P_k = \overrightarrow{P_i^c P_j^c} \cdot \overrightarrow{P_j^c P_k^c} \Big/ \left|\overrightarrow{P_i^c P_j^c}\right| \cdot \left|\overrightarrow{P_j^c P_k^c}\right| \\ \cos\theta = (\overrightarrow{P_i^c P_j^c}) \cdot (\overrightarrow{P_m^c P_k^c}) \Big/ \left|\overrightarrow{P_i^c P_j^c}\right| \cdot \left|\overrightarrow{P_m^c P_k^c}\right| \end{cases}. \tag{3}$$

There are 45 angle constraints aggregately.

To further ensure the shape (preserve the rigidity of the feature points) of the geometric figure, another constraint requires consideration: any triangle can make up a plane, and the remaining two points and the triangle are on the same plane

$$\begin{cases} (\overrightarrow{P_i P_j} \times \overrightarrow{P_i P_m}) \cdot \overrightarrow{P_i P_n} = 0 \\ (\overrightarrow{P_i P_j} \times \overrightarrow{P_i P_m}) \cdot \overrightarrow{P_i P_k} = 0 \end{cases}. \tag{4}$$

Taking all the constraints above into account, the following equations are obtained

$$\begin{cases} e(i,j) = h_i^2 \left|\overrightarrow{O_c I_i}\right|^2 + h_j^2 \left|\overrightarrow{O_c I_j}\right|^2 - 2h_i h_j \overrightarrow{O_c I_i} \cdot \overrightarrow{O_c I_j} - \left|\overrightarrow{P_i P_j}\right|^2 \\ f(i,j,k) = \left(h_j \overrightarrow{O_c I_j} - h_i \overrightarrow{O_c I_i}\right) \cdot \left(h_k \overrightarrow{O_c I_k} - h_j \overrightarrow{O_c I_j}\right) \Big/ \\ \left|h_j \overrightarrow{O_c I_j} - h_i \overrightarrow{O_c I_i}\right| \cdot \left|h_k \overrightarrow{O_c I_k} - h_j \overrightarrow{O_c I_j}\right| - \cos\angle P_i P_j P_k \\ g(i,j,k,m) = \left(h_j \overrightarrow{O_c I_j} - h_i \overrightarrow{O_c I_i}\right) \cdot \left(h_k \overrightarrow{O_c I_k} - h_j \overrightarrow{O_c I_m}\right) \Big/ \\ \left|h_j \overrightarrow{O_c I_j} - h_i \overrightarrow{O_c I_i}\right| \cdot \left|h_k \overrightarrow{O_c I_k} - h_j \overrightarrow{O_c I_m}\right| - \cos\theta \\ h(i,j,m,n) = \left[\left(h_j \overrightarrow{O_c I_j} - h_i \overrightarrow{O_c I_i}\right) \times \left(h_m \overrightarrow{O_c I_m} - h_i \overrightarrow{O_c I_i}\right)\right] \\ \qquad \cdot \left(h_n \overrightarrow{O_c I_n} - h_i \overrightarrow{O_c I_i}\right) \quad . \end{cases} \tag{5}$$

Given that the objective function $h(i,j,m,n)$ converges significantly faster than does the objective functions $e(i,j)$, $f(i,j,k)$, and $g(i,j,k,m)$, and the importance of distance constraints is higher than the angle constraints, two penalty factors M_1 and M_2 are applied. By multiplying the objective function $g(i,j,m,n)$ with M_1 and

multiplying the objective function $g(i,j,m,n)$ with M_2, the unconstrained nonlinear optimization objective function of h_i is created, where $i = 0, 1, 2, 3, 4$.

$$F = M_2 \cdot \sum_{i=0}^{4} \sum_{j=i+1}^{4} e(i,j) + M_1 \cdot \sum_{i=0}^{4} \sum_{\substack{j=i+1 \\ m\neq i,j \\ n\neq i,j,m}}^{4} h(i,j,m,n)$$

$$+ \sum_{i=0}^{4} \sum_{\substack{j=i+1 \\ k\neq i,j}}^{4} \mathrm{f}(i,j,k) + \sum_{i=0}^{4} \sum_{\substack{j=i+1 \\ k\neq i,j \\ m\neq i,j,k}}^{4} g(i,j,k,m) \quad . \quad (6)$$

The Levenberg-Marquardt optimization method is used to solve h_i. The initial value should be provided for the solution of h_i to ensure accuracy and convergence speed of the non-linear algorithm because the entire solution process is nonlinear and iterative.

The scaling and orthography projection model (also known as weak-perspective model) is an approximation of the actual perspective projection model. This approximation can be seen as the synthesis of two projections. Firstly, the entire object is projected toward the plane that is parallel to the image plane in a direction parallel to the optical axis. Then, the object figure on the plane mentioned above is projected toward the image plane of a camera, in accordance with the perspective projection model.

Figure 3 shows that according to the scaling and orthography projection, a plane through No. 0 point parallel to the image plane is drawn, the feature points (from 1 to 4) are projected toward this plane (represented with R_i) in a direction parallel to the optical axis. This plane is at a distance Z_0 from the center of projection O_c. Then, R_i is projected toward the image plane by a perspective projection. The coordinates of the five feature points in the camera coordinate system are $P_i(X_i, Y_i, Z_i)$ and the coordinates of P_i on the image plane in the scaling and orthography projection model can be written as

$$\begin{cases} x_i' = fX_i/Z_0 \\ y_i' = fY_i/Z_0 \end{cases} . \quad (7)$$

Suppose that $w = f/Z_0$, w can be calculated by

$$\begin{cases} a = (P_0P_1 + P_0P_2 + P_1P_2)(-P_0P_1 + P_0P_2 + P_1P_2) \\ \quad (P_0P_1 - P_0P_2 + P_1P_2)(P_0P_1 + P_0P_2 - P_1P_2) \\ b = I_0I_1^2(-P_0P_1^2 + P_0P_2^2 + P_1P_2^2) + I_0I_2^2(P_0P_1^2 - P_0P_2^2 \\ \quad + P_1P_2^2) + I_1I_2^2(P_0P_1^2 + P_0P_2^2 - P_1P_2^2) \\ c = (I_0I_2 + I_1I_2)(-I_0I_1 + I_0I_2 + I_1I_2) \\ \quad \cdot (I_0I_1 - I_0I_2 + I_1I_2)(I_0I_1 + I_0I_2 - I_1I_2) \\ w = \sqrt{\dfrac{b + \sqrt{b^2 - ac}}{a}} \end{cases} , \quad (8)$$

and $1/w$ is set as the initial value of h_i.

In the process of positioning, the camera captures an image of the target each time, and the coordinates of the feature points in the camera coordinate system can be calculated at the current location. The target local coordinate system can be established based on these coordinates. P_0 is set as the origin of the coordinate system, $\overrightarrow{P_2P_4}$ is set as the direction vector of the Y axis, $\overrightarrow{P_0P_1}$ is established as the direction vector of the X axis, and $\overrightarrow{P_2P_4} \times \overrightarrow{P_0P_1}$ is set as the direction vector of the Z axis. Suppose that $\overrightarrow{P_0P_1} = (v_x, v_y, v_z)$, $\overrightarrow{P_2P_4} = (u_x, u_y, u_z)$, and $\overrightarrow{P_2P_4} \times \overrightarrow{P_0P_1} = (w_x, w_y, w_z)$, the rotation and translation matrix can be written as

$$M = R \cdot T = \begin{bmatrix} u_x & u_y & u_z & -u_xx_0 - u_yy_0 - u_zz_0 \\ v_x & v_y & v_z & -v_xx_0 - v_yy_0 - u_zz_0 \\ w_x & w_y & w_z & -w_xx_0 - w_yy_0 - w_zz_0 \\ 0 & 0 & 0 & 1 \end{bmatrix} . \quad (9)$$

The pose of the target in position 1 is $M_1 = R_1 \cdot T_1$, and that of the target in position 2 is $M_2 = R_2 \cdot T_2$. Thus, the pose of the targets from positions 1 to 2 is

$$M = M_2 \cdot M_1^{-1} = R_2T_2 \cdot (R_1T_1)^{-1} \quad . \quad (10)$$

Perspective projection is generally not a shape preserving transformation. Only lines are mapped as lines on the image plane. Two- and three-dimensional objects with a non-zero projection area are distorted if they are not coplanar with the image plane. Perspective projection distorts the shape of the circular features on the image plane depending on the angle and displacement between the object surface and the image plane. Only when the surface and the image plane are parallel to the projections remain circular. Usually the perspective projection of a circle is an ellipse. As shown in Fig. 4, the five circular landmarks are projected toward the image plane and the equation of the projections of five circular landmarks with radius r on the image plane can be expressed with the ideal image coordinates. The centers of the projections (ellipses) and the projection points of the circular landmark centers on the image plane are represented by

$$\begin{cases} x_{ui}^e = (n^2 + p^2 - r^2e^2)(mw + op - der^2) \\ \quad -(mo + np - dFr^2)(nw + pq - eFr^2)/ \\ \quad (mn + op - 2der^2)^2 - (m^2 + o^2 - r^2d^2) \\ \quad (n^2 + p^2 - r^2e^2) \\ y_{ui}^e = (m^2 + o^2 - r^2d^2)(nw + pq - Fer^2) \\ \quad -(mn + op - Fer^2)(mo + oq - dFr^2)/ \\ \quad (mn + op - 2der^2)^2 - (m^2 + o^2 - r^2d^2) \\ \quad (n^2 + p^2 - r^2e^2) \\ x_{ui}^c = \dfrac{(n^2+p^2)(mw + op) - (mo + np)(nw + pq)}{(mn + op)^2 - (m^2 + o^2)(n^2 + p^2)} \\ y_{ui}^c = \dfrac{(m^2+o^2)(nw + pq) - (mn + op)(mo + oq)}{(mn + op)^2 - (m^2 + o^2)(n^2 + p^2)} \end{cases} , \quad (11)$$

where $m = a - dx_{0i}$, $n = b - ex_{0i}$, $w = c - Fx_{0i}$, $o = h - dy_{0i}$, $p = j - ey_{0i}$, $q = k - Fy_{0i}$, $a = r_5t_z - r_8t_y$, $b = r_8t_x - r_2t_z$, $c = fr_2t_y - fr_5t_x$, $d = r_4r_8 - r_5r_7$, $e = r_2r_7 - r_1r_8$, $F = fr_1r_5 - fr_4r_2$, $h = r_4t_z - r_7t_y$, $i = r_7t_x - r_1t_z$, and $k = fr_1t_y - fr_4t_x$; f is the focal length, R and T represent the rotation and translation matrix between the camera coordinate system and the target local coordinate system, respectively. The center of each ellipse $(u_i,\ v_i)$ is extracted by the center of gravity method, then the pose of the target is calculated and

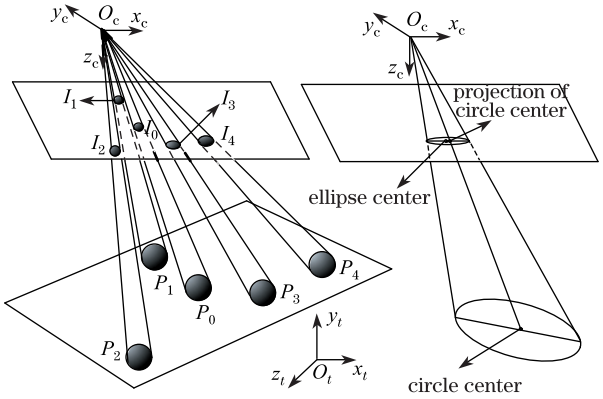

Fig. 4. Perspective projection of five circular landmarks.

the R and T between the target local coordinate system and camera coordinate system is obtained in accordance with part 2. Generally, the ellipse center and projected point of the circle center are not the same. Thus, a bias is induced if the centers of the projections of the circles on the image plane are treated as the projection points of the circular landmarks centers. This bias should be corrected using

$$\begin{cases} x_{di}^e\{1+k[(x_{di}^e)^2+(y_{di}^e)^2]\}=x_{ui}^e \\ y_{di}^e\{1+k[(x_{di}^e)^2+(y_{di}^e)^2]\}=y_{ui}^e \\ x_{di}^c\{1+k[(x_{di}^c)^2+(y_{di}^c)^2]\}=x_{ui}^c \\ y_{di}^c\{1+k[(x_{di}^c)^2+(y_{di}^c)^2]\}=y_{ui}^c \\ u_i'=u_i-s_x(x_{di}^e-x_{di}^c)/d_x \\ v_i'=v_i-(y_{di}^e-y_{di}^c)/d_y \end{cases}, \tag{12}$$

where k represents the lens radial distortion, d_x and d_y are center to center distances between pixels in the row and column directions, respectively, and s_x is the uncertainty image factor. Equation (12) is used to correct the coordinate of each ellipse.

The center, which is changed into $(u_i',\ v_i')$, and the pose of the target are calculated again using the corrected coordinates until the disparity lower than the default value is shown as

$$dis=\left[\sum_{i=0}^{4}(x_{ui}-x_{ui}^c)^2+(y_{ui}-y_{ui}^c)^2\right]/5, \tag{13}$$

where $(x_{ui},\ y_{ui})$ denotes the ideal coordinates of each ellipse center on the image plane. The pose of the target is obtained. The flow chart of the algorithm is shown in Fig. 5.

A monocular vision experimental system consists of a target, a rotation and translation stage, a CCD camera, and a computer. Two images are captured by the CCD camera on different locations, and the pose of the target can be obtained by comparing the two images.

The camera used in this letter is BASLER A631F with a resolution of 1,392 (h) × 1040 (v) pixels, a CCD area of 6.47 (h) × 4.84 (v) (mm), and a pixel size of 0.00465 × 0.00465 (mm). The lens is a Computar 12 mm. The calibration and measurement targets are all 160 × 140 (mm). The translation stage is Zhuo Li Han Guang TSA-200, which is electronically controlled with a travel length of

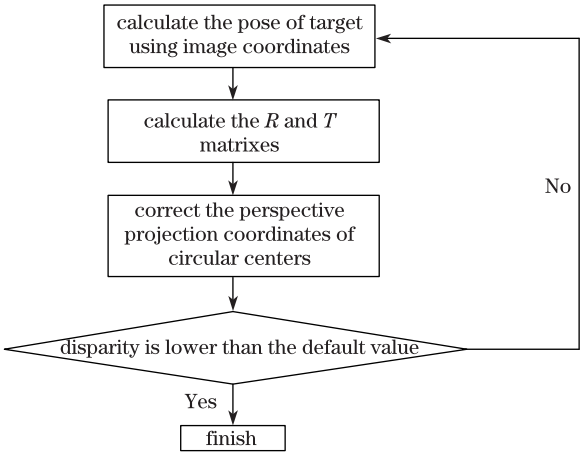

Fig. 5. Flow chart for the iterative calculation of the pose of the target.

200 mm and the repeated positioning accuracy is better than 0.005 mm. The rotation stage RSA-100 (also electronically controlled) with a diameter of 100 mm is installed on the translation stage. Its repeated positioning accuracy is better than 0.005°. The calibration results of camera intrinsic parameters according to the Tsai model[17] are as follows: the focus of lens (f): 12.1797 mm; the uncertainty image factor (s_x): 0.0002825; the radial distortion coefficient of camera lens (k): 0.99793; the center pixel of computer image ($c_x,\ c_y$): (703.05, 455.543).

The target pose measurement experiment is divided into two parts.

1) The measurement experiment on target translation

Through the translation and rotation stage, the image is captured every 4 mm. The distance between the target plane in the current position and the previous position can be obtained. The translation measurement results are shown in Table 1. The experimental results show that the translation positioning accuracy is less than ±0.05 mm in the measurement range of 0–40 mm.

Table 1. Measurement Results of Target Translation

Serial Number	t_x	t_y	t_z	Distance between Location i and Location i+1	Error (mm)	Relative Error (%)
0	−3.875	12.375	420.681			
1	−3.988	12.324	416.671	4.013	0.013	0.33
2	−4.121	12.281	412.681	3.993	−0.007	−1.75
3	−4.238	12.232	408.666	4.016	0.016	0.4
4	−4.367	12.184	404.656	4.012	0.012	0.3
5	−4.477	12.132	400.698	3.960	−0.040	−1
6	−4.591	12.079	396.693	4.007	0.007	1.75
7	−4.728	12.033	392.731	3.964	−0.036	−0.9
8	−4.866	11.982	388.758	3.976	−0.024	−0.6
9	−4.991	11.933	384.766	3.994	−0.006	−0.15
10	−5.118	11.887	380.727	4.041	0.041	1.03

Table 2. Measurement Results of Target Rotation

Serial Number	Position (deg.)	Angle between Location i and Location i+1 (deg.)		
		Calculating Value	Error (deg.)	Relative Error (%)
0	4			
1	10	6.049	0.049	0.82
2	16	6.032	0.032	0.53
3	22	6.029	0.029	0.48
4	28	6.016	0.016	0.27
5	34	5.962	−0.038	−0.63
6	40	5.955	−0.045	−0.75
7	46	5.948	−0.052	−0.87
8	52	5.965	−0.035	−0.58
9	58	5.996	−0.004	−0.067

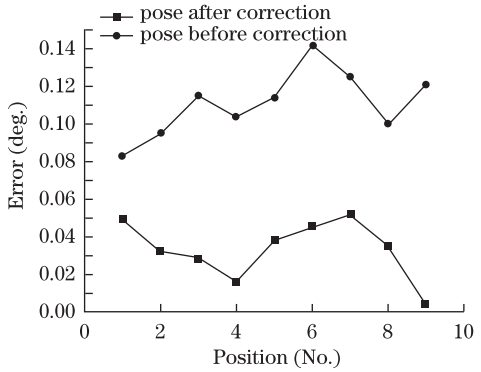

Fig. 6. Rotation poses before and after correction.

2) The measurement experiment on target rotation

The target rotary angle is limited for some feature points and may go beyond the camera's shooting range if the target rotary angle is excessively large. Thus, 60° is set as the limit of target rotation. With the stage rotating 6° each time, the angle between the adjacent positions is calculated in accordance with parts 2 and 3. The results are shown in Table 2. The experimental results show that the rotation positioning accuracy is less than ±0.06° in the measurement range of 4°–60°. To show the effects of correction in part 3, we display the results of the rotation poses before and after correction as shown in Fig. 6.

In conclusion, the pose estimation method based on geometric constraints is studied in this letter. The coordinates of the five feature points in the camera coordinate system can be calculated to obtain the pose of the object on the basis of geometric constraints formed by the feature points and the coordinates of the feature points on the CCD image plane. The scaling and orthography projection model is used to approximate the perspective projection model; the coordinates of the five feature points in the camera coordinate system is obtained on the basis of scaling and orthography projection, and are set as the initial values of the solution process to ensure the accuracy and convergence rate of the non-linear algorithm. In accordance with the perspective projection characteristics of the circular feature landmarks, we propose an approach that enables the iterative acquisition of the accurate pose of targets through the correction of the perspective projection coordinates of the circular feature landmark centers. The experimental results show that the translational positioning accuracy reaches ±0.05 mm in the measurement range of 0–40 mm and rotary positioning accuracy reaches ±0.06° in the measurement range of 4°–60°.

This work was supported by the Important National Science and Technology Specific Project under Grant No. 2009ZX04014-092.

References

1. Y. Fang, D. M. Dawson, W. E. Dixon, and P. Chawda, IEEE Trans. Syst. Man Cybernet **35,** 1041 (2005).
2. F. Tatar, J. Mollinger, and A. Bossche, Proc. IEEE on Sensors 987 (2003).
3. S. Hao, Z. Chai, Z. Zhang, and Y. Hu, Electronics optics and control (in Chinese) **9,** 19 (2002).
4. S. Chen, T. Zhou, X. Zhang, and C. Sun, "Study on the monocular vision measurement system of the position and attitude of the object" (in Chinese), Master Thesis (Tianjin University, 2007).
5. Z. Chao, G. Jiang, W. Huang, S. Song, and Q. Yu, Optics Precision Eng. (in Chinese) **18,** 2044 (2010).
6. T. Jin, H. Jia, and W. Hou, Chin. Opt. Lett. **8,** 601 (2010).
7. E. Paperno, I. Sasada, and E. Leonovich, IEEE Trans. Magnetic Tracking **37,** 1938 (2001).
8. H. Cui, W. Liao, X. Cheng, N. Dai, and T. Yuan, Chin. Opt. Lett. **8,** 33 (2010).
9. M. Maeda, T. Oqawa, K. Kiyokawa, and H. Takemura, in *Proceedings of the Eighth International Symposium on Wearable Computers* 77 (2004).
10. X. Gao, K. Xu, H. Zhang, and X. Liu, Chinese J. Scientific Instrument (in Chinese) **28,** 1479 (2007).
11. D. F. DeMenthon and L. S. Davis, International Journal on Computer Vision **15,** 123 (1995).
12. S. Chen, T. Zhou, X. Zhang, and C. Sun, Chinese J. Sensors and Actuators (in Chinese) **20,** 2011 (2007).
13. M. L. Liu and K. H. Wong, Pattern Recognition Lett. **20,** 69 (1999).
14. Z. Y. Hu and F. C. Wu, Pattern Anal. Mach. Intell. **24,** 550 (2002).
15. J. Tang, W. Chen, and J. Wang, Applied Mathematics and Computation **205,** 628 (2008).
16. J. Heikkilä and O. Silvén, Int. J. Pattern Recognition and Artificial Intelligence **10,** 1066 (1996).
17. C. Sun, L. Tao, and P. Wang, Chin. Opt. Lett. **4,** 282 (2006).